Eur. Phys. J. C 10, 153–157 (1999)
Digital Object Identifier (DOI) 10.1007/s100529900078

THE EUROPEAN PHYSICAL JOURNAL C

Theoretical description of the HERA data on F_2 at low Q^2

A.B. Kaidalov[1], C. Merino[2]

[1] ITEP, B. Cheremushkinskaya 25, 117259 Moscow, Russia
[2] Departamento de Física de Partículas, Universidade de Santiago de Compostela, E-15706 Santiago de Compostela, Spain

Received: 12 August 1998 / Revised version: 12 January 1999 / Published online: 15 July 1999

Abstract. It is shown that the CKMT model for the nucleon structure function F_2 gives a good description of the recent HERA data at low and moderate Q^2. A fit to the same data, obtained with a modified version of the model in which a logarithmic dependence on Q^2 has been included, is also presented. For moderate values of Q^2, in the current available range of x, the first parametrization leads to a better description of the data.

1 Introduction

The CKMT model [1] is a theoretical model based on Regge theory that provides a consistent formulation of the nucleon structure function F_2 in the region of low Q^2 and can be used as a reliable initial condition of the perturbative QCD-evolution equation, to obtain F_2 at larger values of Q^2. Thus, the CKMT model, which gives a good description [1] of all the pre-HERA measurements [2] and of the first small-x experimental data from HERA [3] on $F_2(x,Q^2)$ and $\sigma_{\gamma p}^{\rm tot}(\nu)$, can be useful for investigating the interplay between soft (low Q^2) and hard (high Q^2) physics that is now being studied for the first time in the two small-x experiments (H1 and ZEUS) at HERA.

In this paper, we present the description that the CKMT model provides for the more recent published data on F_2 at low Q^2 by both HERA experiments [4,5]. These data should contribute to a better determination of the initial condition for the perturbative QCD-evolution equation. We also present the description of the experimental data by a modified version of the CKMT model in which a logarithmic dependence on Q^2, asymptotically predicted by perturbative QCD, has been included. The original version of the CKMT model shows much better agreement with experiment in the present experimental range of x and moderate Q^2 than the modified version of the model.

2 The model

Taking into account what is known from Regge theory and hadronic interactions, the CKMT model [1,6] proposes for the nucleon structure functions,

$$F_2(x,Q^2) = F_S(x,Q^2) + F_{NS}(x,Q^2), \tag{1}$$

a parametrization of its two terms in the region of small and moderate Q^2. For the singlet term, corresponding to the Pomeron contribution, the parametrization is

$$F_S(x,Q^2) = A \times x^{-\Delta(Q^2)} \times (1-x)^{n(Q^2)+4} \times \left(\frac{Q^2}{Q^2+a}\right)^{1+\Delta(Q^2)}, \tag{2}$$

with $x \to 0$ behavior determined by an effective intercept of the Pomeron, Δ. The model thus takes into account Pomeron cuts and therefore (and this is one of the main points of the model) depends on Q^2. This dependence is parametrized in [1] as:

$$\Delta(Q^2) = \Delta_0 \times \left(1 + \frac{\Delta_1 \times Q^2}{Q^2+\Delta_2}\right), \tag{3}$$

where Δ_0, Δ_1, and Δ_2 are free parameters which control the change in the effective value of Δ from the region of low Q^2 to that of high Q^2. Thus, for low values of Q^2 (where Regge cuts are important), Δ is close to the effective value found from analysis of hadronic total cross sections ($\Delta \sim 0.08$), while for high values of Q^2 (where the contribution of cuts is small), Δ takes the bare Pomeron value, $\Delta \sim 0.2$–0.25. The parametrization for the nonsinglet term, which corresponds to the secondary Reggeon (f, A_2) contribution, is:

$$F_{NS}(x,Q^2) = B \times x^{1-\alpha_R} \times (1-x)^{n(Q^2)} \times \left(\frac{Q^2}{Q^2+b}\right)^{\alpha_R}, \tag{4}$$

where the $x \to 0$ behavior is determined by the secondary Reggeon intercept α_R, which should be in the range $\alpha_R = 0.4$–0.5. The valence-quark contribution can be separated into the contribution of the u and d valence quarks by the replacement

$$B \times (1-x)^{n(Q^2)} \to B_u \times (1-x)^{n(Q^2)} + B_d \times (1-x)^{n(Q^2)+1}, \tag{5}$$

Table 1. Values of the parameters in the CKMT model obtained in former fits: (a) the fit in which the low Q^2 HERA data [4,5] have also been included; (b) the fit to the same data obtained with the modified version of the CKMT model in which a logarithmic dependence of F_2 on Q^2 has been taken into account; (c) all dimensional parameters, given in GeV^2. The valence counting rules provide the following values of B_u and B_d, for the proton case, when fixing their normalization at $Q_0^2 = 2\mathrm{GeV}^2$: (a) B_u=1.2064, B_d=0.1798; (b) B_u=1.1555, B_d=0.1722; (c) B_u=0.6862, B_d=0.09742. In previous fits, (a), the parameter Δ_1 had been fixed to a value Δ_1=2

CKMT model	(a)	(b)	(c)
A	0.1502	0.1301	0.1188
a	0.2631	0.2628	0.07939
Δ_0	0.07684	0.09663	0.1019
Δ_1	2.0	1.9533	1.2527
Δ_2	1.1170	1.1606	0.1258
c	3.5489	3.5489 (fixed)	3.5489 (fixed)
b	0.6452	0.3840	0.3194
α_R	0.4150	0.4150 (fixed)	0.5872
$\chi^2/d.o.f.$	–	106.95/167	453.19/167

and the normalization condition for valence quarks fixes B_u and B_d at one given value, Q_0^2, of Q^2 (we use $Q_0^2 = 2\mathrm{GeV}^2$ in our calculations). For both the singlet and non-singlet terms, the behavior when x→1 is controlled by $n(Q^2)$,

$$n(Q^2) = \frac{3}{2} \times \left(1 + \frac{Q^2}{Q^2 + c}\right), \qquad (6)$$

chosen in such a way that, for Q^2=0, valence-quark distributions have the same power, given by Regge intercepts, as in the dual parton model [7], $n(0) = \alpha_R(0) - 2\times\alpha_N(0) \sim 3/2$, where $\alpha_N(0)$ is the intercept of the nucleon Regge trajectory, and the behavior of $n(Q^2)$ for large Q^2 coincides with dimensional counting rules [8].

The total cross section for real (Q^2=0) photons can be obtained from the structure function F_2 using the following relation:

$$\sigma_{\gamma p}^{\mathrm{tot}}(\nu) = \left[\frac{4\pi^2\alpha_{EM}}{Q^2} \times F_2(x, Q^2)\right]_{Q^2=0}. \qquad (7)$$

The proper $F_2(x, Q^2) \sim Q^2$ behavior at $Q^2 \to 0$ is fulfilled in the model due to the last factors in equations (2) and (4), which are similar to those in references [9] and [10]. Thus, the $\sigma_{\gamma p}^{\mathrm{tot}}(\nu)$ has the following form in the CKMT model:

$$\sigma_{\gamma p}^{\mathrm{tot}}(\nu) = 4\pi^2\alpha_{EM} \times \left(A \times a^{-1-\Delta_0} \times (2m\nu)^{\Delta_0} + (B_u + B_d) \times b^{-\alpha_R} \times (2m\nu)^{\alpha_R - 1}\right). \qquad (8)$$

The CKMT then parametrizes both the nucleon structure functions and γp total cross sections by an 8-parameter function. Besides the normalizations of the u and d contributions, 4 out of the 8 parameters appear in (8), so the proton structure function contains only 4 extra parameters. Although the parameters are not completely free, and are correlated, some theoretical uncertainty still exists in the determination of their exact values. To eliminate this uncertainty, comparison with experimental data is needed. The CKMT model with the values of the parameters which are listed in Table 1(a) gives [1] a good description of all the experimental data on total cross sections for real photons and nucleon structure functions published by former, pre-HERA experiments [2], and of the first HERA measurements [3]. It should be noted that the values obtained in the fit for the most significant parameters are consistent with the expected values in Regge theory. In addition, the model provides [11,12] reasonable descriptions of the HERA data on diffraction [13] by parametrizing the Pomeron structure function, and also of the available experimental data on nuclear shadowing [14], because of the use of this parametrization of the Pomeron structure function in the frame of the Gribov theory [15].

3 Description of the HERA data on F_2 at low Q^2

In the former fit of reference [1], the accuracy in the determination of the values of the parameters in the model is limited by the lack of experimental data at low and moderate Q^2. The publication of the new experimental data [4,5] on F_2 from HERA at low and moderate Q^2 allows us to include in the fit experimental points situated in the kinematical region where our parametrization should describe the data.

Thus we proceed as in [1], now testing the model in larger regions of x and Q^2 by adding into a global fit the H1 and ZEUS experimental data on F_2 at low and moderate Q^2 to those [2] from the NMC and E665 Collaborations, and to the data on cross sections for real photoproduction. We take as initial conditions for the values of the different parameters those obtained in the previous fit [1]. The result of the new common fit to $\sigma_{\gamma p}^{\mathrm{tot}}$ and F_2 is presented in Figs. 1 and 2, and the final values of the parameters can be found in Table 1(b). Now the parameter Δ_1 (fixed to Δ_1=2. in [1]) is left free, and, since the fit turns out not to be very sensitive to changes in the values of the parameters c and α_R, these parameters are fixed to their original values in [1]. As can be seen in the figures, the quality of the description provided by the CKMT model of all the experimental data, and, in particular, of the new HERA data, is very good, with a value of χ^2/d.o.f. = 106.95/167 for the global fit, with the statistical and systematic errors treated in quadrature, and with the relative normalization among all the experimental data sets equal to 1.

Also, since the small-x HERA experiments allow for the first time the study of the interplay between soft and hard physics, we have modified our model, with basically only power dependence on Q^2, to include a logarithmic dependence on Q^2, as predicted asymptotically by perturbative QCD [16]. Our aim is to investigate whether

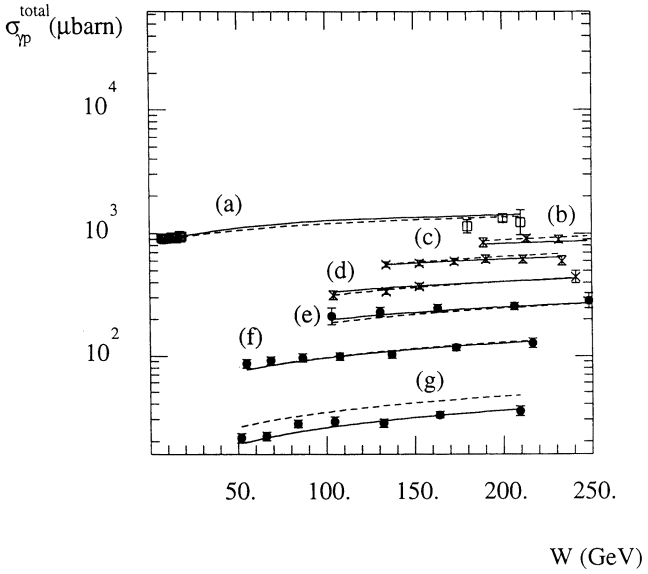

Fig. 1. $\sigma_{\gamma p}^{\rm tot}$ and $\sigma_{\gamma^* p}^{\rm tot}$ (in μ barns) vs W (in GeV) for different values of Q^2. Theoretical fits have been obtained with the CKMT model (full line) and the modified version of the CKMT model (dashed line). Points at (a) $Q^2 = 0\text{GeV}^2$ (*8.); (b) $Q^2 = 0.15\text{GeV}^2$ (*6.); (c) $Q^2 = 0.25\text{GeV}^2$ (*5.); (d) $Q^2 = 0.5\text{GeV}^2$ (*4.); (e) $Q^2 = 0.8\text{GeV}^2$ (*3.); (f) $Q^2 = 1.5\text{GeV}^2$ (*2.); and (g) $Q^2 = 3.5\text{GeV}^2$ (*1.). Experimental points for F_2 ($\sigma_{\gamma^* p}^{\rm tot}$) are from [4] (black circles), and [5] (crosses), and experimental data on $\sigma_{\gamma p}^{\rm tot}$ are from [20,21,22]. Experimental points from NMC and E665 are not presented in this figure for the sake of clarity, but the quality of the fit to these points does not change from [1]

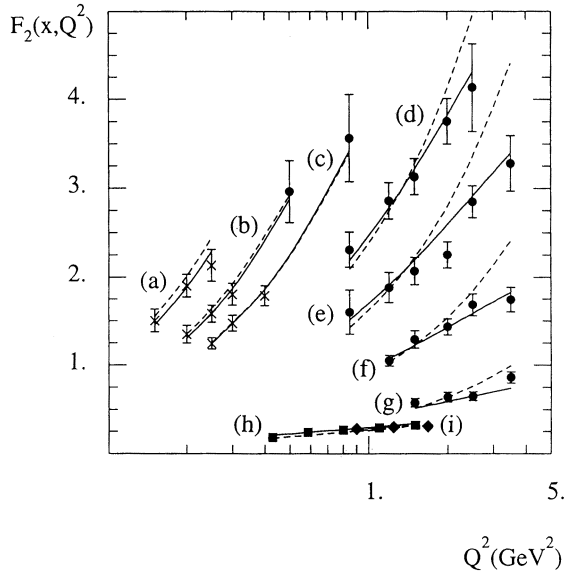

Fig. 2. $F_2(x, Q^2)$ vs. Q^2 (in GeV^2) for different values of x. Theoretical fits have been obtained with the CKMT model (full line) and the modified version of the CKMT model (dashed line). Experimental points at (a) from left to right, x=0.42×10^{-5}, x=0.44×10^{-5}, and x=0.46×10^{-5} (*8.); (b) from left to right, x=0.85×10^{-5}, x=0.84×10^{-5}, x=0.83×10^{-5}, and x=0.86×10^{-5} (*6.); (c) from left to right, x=0.13×10^{-4}, and three points at x=0.14×10^{-4} (*5.); (d) x=0.5×10^{-4} (*4.); (e) x=0.8×10^{-4} (*3.); (f) x=0.2×10^{-3} (*2.); (g) x=0.5×10^{-3} (*1.); (h) x=0.52×10^{-2} (*1.); and (i) x=0.13×10^{-1} (*1.). Experimental points for F_2 are from [4] (black circles), [5] (crosses), and [2] (black squares for the E665 points, and black diamonds for the NMC points)

such a modified version of the model provides a smoother matching in the description of both the soft and the hard regimes, and whether the available experimental data can distinguish a description where the Q^2 dependence saturates from that of a model without such a saturation.

To include the logarithmic dependence on Q^2 in our model, we take into account that the behavior of F_2 at small x is given in QCD by the singularities of the moments of the structure functions [17], the rightmost singularity giving the leading behavior. Thus we introduce into (1) the following factors [17,18], which correspond to the moments of the structure functions in the language of the OPE expansion, and can be calculated by the convolution in rapidity of the hard-upper part with the soft-lower part of the leptoproduction diagram:

$$\left(\frac{\alpha_s(Q_0^2)}{\alpha_s(Q^2)}\right)^{d_i(n_i)}, \; i = S, NS, \tag{9}$$

where the strong coupling constant is taken as

$$\alpha_s(Q^2) = \frac{4\pi}{\beta_0 \times \log\left(\frac{Q^2+M^2}{\Lambda^2_{\rm QCD}}\right)}, \tag{10}$$

where $M \sim 1$GeV, a hadronic mass [19] is included in (10) to avoid the singularity in α_s when $Q^2 \to \Lambda^2_{\rm QCD}$, $\Lambda_{\rm QCD} = 0.2$GeV, and $\beta_0 = 11 - 2/3 n_f$ (we use in our calculations a number of flavors n_f=3). The exponents $d_S(n_S)$ and $d_{NS}(n_{NS})$ in (9) are proportional to the largest eigenvalue of the anomalous dimension matrix, and to the anomalous dimension, respectively:

$$d_S(n_S) \sim \frac{d_0}{4(n_S - 1)} - d_1, \tag{11}$$

with

$$d_0 = \frac{48}{\beta_0}, d_1 = \frac{11 + 2/27 n_f}{\beta_0},$$

and

$$d_{NS}(n_{NS}) = \frac{16}{33 - 2n_f} \times \left(\frac{1}{2n_{NS}(n_{NS}+1)} + \frac{3}{4} - S_1(n_{NS})\right), \tag{12}$$

with

$$S_1(n_{NS}) = n_{NS} \times \sum_{k=1}^{\infty} \frac{1}{k(k + n_{NS})}.$$

Thus (1) is modified in the following way:

$$F_2(x, Q^2) = \left(\frac{\alpha_s(Q_0^2)}{\alpha_s(Q^2)}\right)^{d_S(n_S)}$$

$$\times F_S(x,Q^2) + \left(\frac{\alpha_s(Q_0^2)}{\alpha_s(Q^2)}\right)^{d_{NS}(n_{NS})} \times F_{NS}(x,Q^2). \quad (13)$$

The exponents of the new factors in (13), $d_S(n_S)$ and $d_{NS}(n_{NS})$, give us the singularities in n_i, $i = S$, NS, of the momenta, which, as we mentioned above, control the QCD small-x behavior of F_2. Therefore, these exponents have to be evaluated in our model at $n_S = 1 + \Delta(Q^2 \to \infty) = 1 + \Delta_0(1 + \Delta_1)$ and $n_{NS} = \alpha_R$, respectively (see (2) and (4)). We consider in our expressions only the LO behavior, and again we can use the relation (3) to obtain from (13) the expression of the total cross section for real photoproduction.

At this point, two main differences between our approach and that of [18], which also provides good fits of the experimental data, can be mentioned. First, while in our model just one Pomeron with a Q^2-dependent intercept is present, in the approach of [18], two components, a constant soft Pomeron and a hard Pomeron with a very large intercept $\Delta \sim 0.5$, are used. Second, in our case the proper Q^2 behavior of F_2 (see also [10]) for $Q^2 \to 0$ is provided in a natural way, and thus a justified choice [19] of the effective mass M^2 in $\alpha_s(Q^2)$ (see (10)) provides a nonsingular behavior of $\alpha_s(Q^2)$ throughout the Q^2 range when the logarithmic dependence on Q^2 is added. In [18], on the contrary, one particular value of $M^2 = \Lambda^2_{\rm QCD}$ has to be taken in (10) in order to get the required behavior of F_2 for $Q^2 \to 0$, resulting in a singular behavior $\alpha_s(Q^2) \to \infty$ as $Q^2 \to 0$.

Now we repeat the fit with the modified version of the CKMT model. Again we take as starting point for the QCD evolution the value $Q_0^2 = 2\text{GeV}^2$, used to fix the normalization of the valence component. The result of this second fit is also presented in Figs. 1 and 2, and the final values of the parameters in the model are given in Table 1(c). In this case, only the parameter c was fixed to its value in [1].

As it can be seen in the figures, the quality of this second fit is substantially worse than for the original model, the value of $\chi^2/\text{d.o.f.} = 453.19/167$ now being appreciably higher than in the fit obtained with the nonmodified version of the CKMT model. Note that the two models are essentially different only for $Q^2 \geq 1$ GeV^2, since α_s is practically constant at lower values of Q^2, and that by an appropiate choice of free parameters, it is possible to obtain nearly identical predictions for both models in this low Q^2 region. However, for values of $Q^2 \geq 1$ GeV^2, there is no freedom in the modified version of the model, which predicts a fast increase of the structure functions with Q^2, as compared with the original version of the model. This behavior contradicts experiment in this region. We think that this is instructive, as it illustrates two important points. First, the asymptotic formulas for a solution of QCD-evolution equations used in the second parametrization are valid at much smaller values of x than those in the region studied at HERA (see discussion of this point in [6]). Secondly (and, we believe, more importantly), an extrapolation of the Q^2 dependence based on QCD evolution from a region of large Q^2 to a region where $Q^2 \leq 2\text{GeV}^2$ leads to too- large values of $\text{d}F_2/\text{dln}Q^2$ as compared to HERA experimental data, indicating a change of the dynamics in this region. This fact is also illustrated by a comparison of the Q^2 derivatives for the second parametrization to experimental data in Fig. 2. On the contrary, the purely nonperturbative original parametrization reproduces satisfactorily these derivatives in the whole region of $Q^2 \leq 3$–4 GeV^2.

One common feature of the two fits is that they give values of the total cross section for real photons that are higher than the experimental ones in the region of large W, where the experimental error bars are large. More accurate measurements in this region should clarify this point. Concerning the final values of the parameters, it should be noted that Δ_0 takes similar values in cases (b) and (c), both slightly larger than the original value in (a), providing a stable asymptotic behavior of the effective $\Delta(Q^2 \to \infty) \sim 0.25$–$0.3$, which includes some effects of perturbative QCD evolution.

4 Conclusions

In conclusion, the CKMT model for the parametrization of the nucleon structure functions provides a very good description of all the available experimental data on $F_2(x,Q^2)$ at low and moderate Q^2, including the more recent small-x HERA points. In addition, the fit to the same data, obtained with a modified version of the model in which a logarithmic dependence on Q^2 is included, has been presented. The χ^2/d.o.f. of this second description is appreciably higher than that of the fit obtained with the nonmodified version of the CKMT model.

Acknowledgements. We are grateful to K.G. Boreskov, A. Capella, G. Parente, Yu. A. Simonov and R. Vázquez for useful discussions. One of us (C.M.) also wants to thank the ITEP members for their kind hospitality during the realization of this work.

References

1. A. Capella, A.B. Kaidalov, C. Merino, J. Trân Than Vân, Phys. Lett. B **337**, 358 (1994)
2. New Muon Collaboration, P. Amaudruz, et al., Phys. Lett. B **259**, 159 (1992); E665 Collaboration, M.R. Adams, et al., FERMILAB-Pub 1995/396
3. H1 Collaboration, I. Abt, et al., Nucl. Phys. B **407**, 515 (1993); ZEUS Collaboration, M. Derrick, et al., Phys. Lett. B **316**, 412 (1993)
4. H1 Collaboration, C. Adloff, et al. Nucl. Phys. B **497**, 3 (1997)
5. ZEUS Collaboration, J. Breitweg, et al., Phys. Lett. B **407**, 432 (1997)
6. A.B. Kaidalov, "Survey in High Energy Physics", **9**, 143 (1996)
7. A. Capella, U. Sukhatme, C.-I. Tan, J. Trân Than Vân, Phys. Rep. **236**, 225 (1994)

8. S. J. Brodsky, G. Farrar, Phys. Rev. Lett. **31**, 1153 (1973); V. Matveev, R. Muradyan, A. Tavkhelidze, Nuovo Cim. **7**, 179 (1993)
9. H. Abramowicz, E.M. Levin, A. Levy, U. Maor, Phys. Lett. B **269**, 465 (1991)
10. A. Donnachie, P.V. Landshoff, Z. Phys. C **61**, 139 (1994)
11. A. Capella, A.B. Kaidalov, C. Merino, J. Trân Than Vân, Phys. Lett. B **343**, 403 (1995); A. Capella, A.B. Kaidalov, C. Merino, D. Pertermann, J. Trân Thanh Vân, Phys. Rev. D **53**, 2309 (1996)
12. A. Capella, A.B. Kaidalov, C. Merino, D. Pertermann, J. Trân Thanh Vân, Eur. Phys. J. C **5**, 111 (1998)
13. H1 Collaboration, T. Ahmed, et al., Nucl. Phys. B **429**, 477 (1994); H1 Collaboration, T. Ahmed, et al., Phys. Lett. B **348**, 681 (1995); ZEUS Collaboration, M. Derrick, et al., Phys. Lett. B **315**, 481 (1993); B **332**, 228 (1994); B **338**, 477 (1994); ZEUS Collaboration, B. Foster, in Proceedings of the Workshop on Deep Inelastic Scattering and QCD: DIS '95, Paris, France, 1995, edited by J.F. Laporte, Y. Sirois, p. 57
14. M. Arneodo, Phys. Reports **240**, 301 (1994) (and references therein)
15. V.N. Gribov, ZhETF **57**, 654 (1967) [Sov. Phys. JETP **26**, 14 (1968)]
16. Yu.L. Dokshitzer, D.I. Dyakonov, S.I. Troyan, Phys. Rep. **58 (5)**, 269 (1980)
17. A. de Rújula, et al., Phys. Rev. D **10**, 1649 (1974)
18. F. Barreiro, C. López, F.J. Ynduráin, Z. Phys. C **72**, 561 (1996); K. Adel, F. Barreiro, F.J. Ynduráin, Nucl. Phys. B **495**, 221 (1997)
19. Yu. A. Simonov, Yad. Fiz. **58**, 113 (1995) (Phys. At. Nucl. **58**, 107 (1995))
20. D.O. Caldwell, et al., Phys. Rev. Lett. **40**, 1222 (1978)
21. ZEUS Collaboration, M. Derrick, et al., Phys. Lett. B **293**, 465 (1992); ZEUS Collaboration, M. Derrick, et al., Z. Phys. C **63**, 391 (1994)
22. H1 Collaboration, S. Aid, et al., Z. Phys. C **69**, 27 (1995)